

Light-quark meson spectrum in the covariant oscillator quark model with one-gluon-exchange effects

Shin Ishida and Kenji Yamada

Atomic Energy Research Institute, College of Science and Technology, Nihon University, Tokyo 101, Japan

(Received 23 October 1985; revised manuscript received 2 June 1986)

The covariant oscillator quark model, which was extended recently to include one-gluon-exchange effects, is applied to investigate the mass spectrum of light-quark mesons. In the meson rest frame our effective potential due to one-gluon exchange is given as the sum of a Coulomb-type, orbit-orbit-like, spin-orbit, and hyperfine interaction, and has similar general features as in the standard nonrelativistic quark model. However, there are essential differences between them. First, our scheme is manifestly covariant and the potential is concerned with the squared masses of hadrons. Second, our effective one-gluon-exchange potential is greatly modified due to the covariant nature and the retardation effect. Owing to these modifications our model reproduces quite well the experimental behavior of the spectra of radially excited states as well as orbitally excited states.

I. INTRODUCTION

Recently there seems to be no doubt that quantum chromodynamics (QCD) plays an important role as a theoretical basis for the strong hadron interactions. Actually the success of nonrelativistic (NR) quark potential models, being guided by QCD, have become more remarkable than before, especially for heavy-quark systems.¹ They also seem to work well even for light-quark systems,² where the quark motion is highly relativistic. However, their application should be, in principle, limited to static problems, such as mass spectra, magnetic moments, and transition reactions between hadrons with a small mass difference, reflecting the nonrelativistic character of the model, where the effect due to relativistic motion of hadrons as a whole is difficult to include. This difficulty still remains in the recent semirelativistic attempts³ which can, by taking into account the effects of relativistic quark motion properly, describe the spectra of light- and heavy-quark systems in a unified way. The difficulty is most seriously seen in treating electromagnetic processes of hadrons, where it is indispensable to get the conserved effective currents in terms of "observable" hadrons themselves, and in doing so the covariant description of the center-of-mass motion of hadrons is necessary.

This point has been one of the most important motives for the covariant oscillator quark model^{4,5} (COQM), where hadrons themselves are unambiguously defined as Fierz components of multilocal fields (which satisfy a covariant equation heuristically obtained), and the conserved effective hadron currents are given explicitly.

The COQM has a long history of development. However, it has, thus far developed, such shortcomings as the fact that (i) the equation of motion was set up quite arbitrarily and (ii) the treatment was limited in the symmetrical case where the effects of unequal quark masses and of one-gluon exchange (OGE) were neglected. Recently we have improved this situation to some extent. First, by considering⁶ a "prototype" classical mechanics for a con-

finer multiquark system with unequal quark masses, we have derived a space-time equation of hadrons with some physical reasons. Second, we have extended the model so as to include the OGE effects^{5,7,8} in a manifestly covariant way. This scheme has been applied with considerable success to the analyses of the baryon magnetic moments,⁹ of the radiative transitions⁷ of light-quark ground-state mesons, and of the electromagnetic form factors⁵ of mesons and baryons.

In this paper we shall present the results^{5,8} of application of this extended scheme to investigation of the light-quark meson spectra. In Sec. II we give a brief review of our COQM. In Sec. III we describe how to introduce the OGE effects and give the form of the effective potential. In Sec. IV we give our numerical results of the meson spectra and compare them with experiment. In Sec. V we discuss some specific features to our scheme. In the final section some concluding remarks are given.

II. COVARIANT OSCILLATOR QUARK MODEL

In this section we shall review briefly the COQM so far as required for our present application. In this scheme the mesons of quark-antiquark systems are generally described as a bilocal field (wave function)

$$\Phi_{(p)\alpha}^{\beta}(x_1, x_2), \quad (2.1)$$

where x_1 (x_2) is the Lorentz four-vector representing the space-time coordinate of a constituent quark (antiquark), α (β) represents a spinor corresponding to the spin of a quark (antiquark), and the flavor and color indices are omitted for simplicity. The respective parts of the wave function, the spin and the space-time wave function, are covariantly extended, separately, from the corresponding parts of the NR one. Concerning the spin part, there have been proposed two typical ways: the Bargmann-Wigner (BW) scheme¹⁰ using Dirac spinors ($\alpha, \beta = 1-4$), and the minimally boosted Pauli (MP) scheme¹¹ using Pauli spinors ($\alpha, \beta = 1, 2$ and $p = 1, 2$, which is needed only in the

MP scheme). Both schemes give identical results in the present application, where only the wave function in the hadron rest frame is considered.

Concerning the space-time part it is supposed⁶ to satisfy the equation

$$\left[\sum_{i=1}^2 \frac{1}{2m_i} \frac{\partial^2}{\partial x_{i\mu}^2} - U(x_1, x_2) \right] \Phi(x_1, x_2) = 0, \quad (2.2)$$

where m_1 (m_2) is the parameter corresponding to quark (antiquark) mass, and the potential U consists of two parts:

$$U = U_0 + U_G. \quad (2.3)$$

Here the first term U_0 is a confinement potential taken to be a four-dimensional harmonic oscillator, and the second term U_G is a perturbative potential representing the OGE effects which will be specified in Sec. III. It may be worthwhile to note that our basic equation (2.2) is naturally derived by considering the classical "prototype" relativistic mechanics for a confined multiparticle system.

Equation (2.2) is rewritten, in terms of the center-of-mass coordinates and the relative coordinates defined by

$$X_\mu \equiv \frac{1}{m_1 + m_2} (m_1 x_{1\mu} + m_2 x_{2\mu}), \quad x_\mu \equiv x_{1\mu} - x_{2\mu}, \quad (2.4)$$

as

$$\left[\frac{\partial^2}{\partial X_\mu^2} - \mathcal{M}^2(x) \right] \Phi(X, x) = 0 \quad (2.5)$$

with the squared-mass operator of the form

$$\mathcal{M}^2 = dH = d \left[-\frac{1}{2\mu} \frac{\partial^2}{\partial x_\mu^2} + U(x) \right], \quad (2.6a)$$

$$d = 2(m_1 + m_2), \quad \mu = \frac{m_1 m_2}{m_1 + m_2}. \quad (2.6b)$$

Here it is to be noted that H has a similar form to the energy of relative motion in the NR potential model except for now using Lorentz four-vectors instead of three-vectors.

In order to "freeze" the redundant freedom of relative time, we suppose the definite-metric-type subsidiary condition¹² holds for the unperturbed wave function

$$P_\mu a_\mu^\dagger \Phi = 0, \quad (2.7)$$

where P_μ is the four-momentum of the center-of-mass motion, and a_i^\dagger (a_i) is the creation (annihilation) operator for internal oscillations. As is well known, the wave function which satisfies the physical state condition of Eq. (2.7) is normalizable and gives¹³ the desirable asymptotic behavior of electromagnetic form factors of hadrons.

Thus our scheme transforms the results of the NR potential model for the linear masses of hadrons to the ones for squared masses, keeping Lorentz covariance. As an important result we get linear orbital Regge trajectories, as is desired, for the squared masses of hadrons in the unperturbed limit. We shall see later that the OGE effects change little the linearity of leading Regge trajectories. Experimentally this linearity is known to be valid up to

the very high orbitally excited states, as will be shown in Sec. IV.

III. COVARIANT ONE-GLUON-EXCHANGE POTENTIAL

In this section we derive our general formula for the squared masses of mesons including OGE effects treated as a first-order perturbation. Since there has not been developed any established method of covariant perturbation for confined bound systems, we are forced to proceed heuristically in the following.

Our squared-mass operator of Eq. (2.6a) consists of, corresponding to Eq. (2.3), two parts:

$$\mathcal{M}^2 = \mathcal{M}_0^2 + \delta \mathcal{M}_G^2, \quad (3.1)$$

where

$$\mathcal{M}_0^2 = dH_0 = d \left[-\frac{1}{2\mu} \frac{\partial^2}{\partial x_\mu^2} + U_0(x) \right], \quad (3.2a)$$

$$\delta \mathcal{M}_G^2 = dU_G. \quad (3.2b)$$

For the confinement potential we assume

$$U_0 = C + \frac{1}{2} K x_\mu^2, \quad (3.3)$$

where C and K are flavor-dependent constants. Then the unperturbed squared masses are given by

$$(M_0^{(N)})^2 = (M_0^{(0)})^2 + N\Omega, \quad (3.4)$$

with

$$(M_0^{(0)})^2 = dC + \Omega, \quad (3.5a)$$

$$\Omega = d \left[\frac{m_1 + m_2}{m_1 m_2} K \right]^{1/2}, \quad (3.5b)$$

where N is the number of excitations and Ω^{-1} gives the slope of orbital Regge trajectories.

A. Introduction of OGE effects

In order to take into account the OGE effects covariantly, we start from the corresponding effective action^{7,8} to the OGE potential:

$$I_G = - \int d^4 x_1 d^4 x_2 \bar{\Phi} \delta \mathcal{M}_G^2 \Phi, \quad (3.6)$$

$$\delta \mathcal{M}_G^2 \equiv \frac{d}{F} \Gamma_{1\mu}(x_1) D_{\mu\nu}(x_1 - x_2) \Gamma_{2\nu}(x_2), \quad (3.7)$$

where $\Gamma_{i\mu}$ is a quark-gluon vertex operator, $D_{\mu\nu}$ is a gluon propagator, and F is a flavor-dependent constant with the dimension of mass, which is introduced so as to give the correct dimension to Eq. (3.6) [note that the factor d in Eq. (3.7) necessarily comes from our basic equation (2.2)]. For the vertex operator we assume, in analogy with the conserved effective electromagnetic current⁶ of hadrons, the form

$$\Gamma_{i\mu} = \Gamma_{i\mu}^E + \Gamma_{i\mu}^M, \quad (3.8)$$

$$\Gamma_{i\mu}^E \equiv -ig \left[\frac{\lambda_i^a}{2} \right] \frac{1}{2m_i} \frac{\vec{\partial}}{\partial x_{i\mu}}, \quad (3.9a)$$

$$\Gamma_{\mu}^M \equiv g \left[\frac{\lambda_i^a}{2} \right] \frac{h_M}{2m_i} \sigma_{\mu\nu}^{(i)} \left[\frac{\vec{\partial}}{\partial x_{i\nu}} + \frac{\overleftarrow{\partial}}{\partial x_{i\nu}} \right], \quad (3.9b)$$

where the derivative operator is concerned only with Φ or $\bar{\Phi}$, g is the effective quark-gluon coupling constant, λ_i^a is the color-SU(3) matrix, and h_M is a dimensionless parameter corresponding to the effective quark color-magnetic moment (in the case of the normal moment, $h_M=1$). There can be a large anomalous interaction¹⁴ due to the gluon self-interaction, and it may be generally flavor dependent.¹⁵ In Eq. (3.9b) the spin matrices $\sigma_{\mu\nu}^{(i)}$'s are defined as

$$\sigma_{\mu\nu}^{(1)} = \frac{1}{2i} [\gamma_\mu^{(1)}, \gamma_\nu^{(1)}], \text{ etc. ,}$$

in the BW scheme, and

$$\sigma_{ij}^{(1)} = \epsilon_{ijk} \sigma_k^{(1)}, \quad \sigma_{i4}^{(1)} = \rho_i \sigma_i^{(1)} = -\sigma_{4i}^{(1)}, \text{ etc.}$$

(where ρ_i 's and σ_i 's are the Pauli matrices that are mutually commuting) in the MP scheme, respectively (it should be understood for an antiquark $\sigma_{\mu\nu}^{(2)} \rightarrow -\sigma_{\mu\nu}^{(2)T}$, A^T denoting the transpose of A), and $\bar{\Phi} = \Phi^\dagger \gamma_4^{(1)} \gamma_4^{(2)T}$ in the BW scheme and $\bar{\Phi} = \Phi^\dagger \rho_3$ in the MP scheme. Here the first (second) term in Eq. (3.8) is just a covariant generalization of the NR color-convection (spin) current.

As the gluon propagator $D_{\mu\nu}(x)$ [$\equiv \delta_{\mu\nu} D(x)$] we choose¹⁶ the mean of the retarded and the advanced

Green's function D_R and D_A ,

$$\bar{D}(x) = \frac{1}{2} [D_R(x) + D_A(x)] = \text{Re} D_F(x), \quad (3.10)$$

which is equal to the principal part of the Feynman propagator D_F . The explicit forms of these functions are

$$\bar{D}(x) = -\frac{1}{4\pi} \delta(x^2), \quad (3.11a)$$

$$D_R(x) = -\frac{1}{2\pi} \theta(x_0) \delta(x^2) = -\frac{1}{4\pi r} \delta(r-t), \quad (3.11b)$$

$$D_A(x) = -\frac{1}{2\pi} \theta(-x_0) \delta(x^2) = -\frac{1}{4\pi r} \delta(r+t), \quad (3.11c)$$

where $r = |\mathbf{x}|$ and $t = x_0$. There are several plausible reasons for this choice of the gluon propagator: Choosing the Feynman propagator makes $\delta \mathcal{M}_G^2$ complex generally, and the choice $D(x) = \text{Re} D_F(x)$ seems to be implied by the gluon confinement. Furthermore, taking the symmetric combination of D_R and D_A is natural for the physical situation of confined systems, since for such systems the relative time may not be observed [the subsidiary condition of Eq. (2.7) is also consistent with this requirement]. It is also shown that the invariance under particle-antiparticle conjugation leads to the symmetric combination.

By substituting the expression of Γ_μ , Eqs. (3.9a) and (3.9b), into the action of Eq. (3.6) we obtain the squared-mass operator corresponding to the OGE effects as

$$\delta \mathcal{M}_G^2 = \delta \mathcal{M}_{GE}^2 + \delta \mathcal{M}_{GEM}^2 + \delta \mathcal{M}_{GM}^2, \quad (3.12)$$

$$\delta \mathcal{M}_{GE}^2 \equiv -f_c \frac{d}{F} \frac{g^2}{4m_1 m_2} \left[4\bar{D} \frac{\partial^2}{\partial x_{1\mu} \partial x_{2\mu}} + 2 \left[\frac{\partial \bar{D}}{\partial x_{1\mu}} \frac{\partial}{\partial x_{2\mu}} + \frac{\partial \bar{D}}{\partial x_{2\mu}} \frac{\partial}{\partial x_{1\mu}} \right] + \frac{\partial^2 \bar{D}}{\partial x_{1\mu} \partial x_{2\mu}} \right], \quad (3.13a)$$

$$\delta \mathcal{M}_{GEM}^2 \equiv i f_c \frac{d}{F} \frac{g^2 h_M}{4m_1 m_2} \left[2 \left[\sigma_{\mu\nu}^{(1)} \frac{\partial \bar{D}}{\partial x_{1\nu}} \frac{\partial}{\partial x_{2\mu}} + \sigma_{\mu\nu}^{(2)} \frac{\partial \bar{D}}{\partial x_{2\nu}} \frac{\partial}{\partial x_{1\mu}} \right] + (\sigma_{\mu\nu}^{(1)} + \sigma_{\nu\mu}^{(2)}) \frac{\partial^2 \bar{D}}{\partial x_{1\nu} \partial x_{2\mu}} \right], \quad (3.13b)$$

$$\delta \mathcal{M}_{GM}^2 \equiv f_c \frac{d}{F} \frac{g^2 h_M^2}{4m_1 m_2} \sigma_{\mu\nu}^{(1)} \sigma_{\mu\lambda}^{(2)} \left[\frac{\partial^2 \bar{D}}{\partial x_{1\nu} \partial x_{2\lambda}} \right], \quad (3.13c)$$

where the factor $f_c = -\frac{4}{3}$ is due to the color degree of freedom for the singlet $q\bar{q}$ system, and each term in Eq. (3.12) corresponds to the combination of the vertex operators in Eq. (3.8), $\Gamma^E \Gamma^E$, $\Gamma^E \Gamma^M$, and $\Gamma^M \Gamma^M$, respectively.

B. Covariant OGE potential

The unperturbed meson wave function can be written as

$$\Phi(x_1, x_2) = N e^{iP \cdot X} \Psi(x; P), \quad (3.14)$$

where X_μ, x_μ are the center-of-mass and the relative coordinates defined by Eq. (2.4), respectively, P_μ is the center-of-mass momentum, and N is a normalization constant for the plane wave. Then Eq. (3.6) is represented by the internal wave function $\Psi(x; P)$ as

$$\int d^4 x_1 d^4 x_2 \bar{\Phi}(x_1, x_2; P') \delta \mathcal{M}_G^2 \Phi(x_1, x_2; P) = (2\pi)^4 \delta^4(P - P') |N|^2 \int d^4 x \bar{\Psi}(x; P') U_G(x, \vec{\partial}, \overleftarrow{\partial}; P, P') \Psi(x; P), \quad (3.15)$$

where P (P') is the momentum of an initial- (final-) state meson and $\partial_\mu \equiv \partial/\partial x_\mu$.

By using the explicit forms of the vertex operator [Eq. (3.8)] and the propagator [Eq. (3.10)] in the meson rest frame we obtain the OGE potential

$$U_G = U_{GE} + U_{GEM} + U_{GM} \quad (3.16)$$

with

$$U_{GE} = f_c \frac{\alpha_s}{F} \delta(x^2) \left[\frac{(M_0 + M'_0)^2}{4(m_1 + m_2)^2} + \frac{1}{4m_1 m_2} \left[2 \frac{\bar{\partial}}{\partial x_\mu} \frac{\bar{\partial}}{\partial x_\mu} - \frac{\bar{\partial}^2}{\partial x_\mu^2} - \frac{\bar{\partial}^2}{\partial x_\mu^2} \right] \right], \quad (3.17a)$$

$$U_{GEM} = i f_c \frac{\alpha_s}{F} \delta(x^2) \frac{h_M}{2m_1 m_2} (\boldsymbol{\sigma}_1 + \boldsymbol{\sigma}_2) \cdot (\vec{\nabla} \times \vec{\nabla}), \quad (3.17b)$$

$$U_{GM} = f_c \frac{\alpha_s}{F} \delta(x^2) \frac{h_M^2}{4m_1 m_2} [\boldsymbol{\sigma}_1 \cdot \boldsymbol{\sigma}_2 (\vec{\nabla} + \vec{\nabla})^2 - \boldsymbol{\sigma}_1 \cdot (\vec{\nabla} + \vec{\nabla}) \boldsymbol{\sigma}_2 \cdot (\vec{\nabla} + \vec{\nabla})], \quad (3.17c)$$

where $\alpha_s = g^2/4\pi$ is the strong-interaction fine-structure constant and M_0 (M'_0) is the unperturbed mass of an initial- (final-) state meson. In deriving these expressions we used the facts that in our covariant spin scheme the small component of the spin wave function vanishes in the meson rest frame and that the relative-time wave function is always in the ground state due to the subsidiary condition Eq. (2.7).

Changing the “left” derivatives into “right” ones by partial integration we can rewrite the OGE potential into the familiar form

$$U_G = U_C + U_{OO} + U_{SO} + U_T + U_{SS}, \quad (3.18)$$

where

$$U_C = \frac{(M_0 + M'_0)^2}{4(m_1 + m_2)^2} v, \quad (3.19a)$$

$$\begin{aligned} U_{OO} &= -\frac{1}{m_1 m_2} \left[v \frac{\partial^2}{\partial x_\mu^2} + \frac{\partial v}{\partial x_\mu} \frac{\partial}{\partial x_\mu} + \frac{1}{4} \frac{\partial^2 v}{\partial x_\mu^2} \right] \\ &= -\frac{1}{m_1 m_2} \left[v \nabla^2 + \frac{1}{r} \frac{\partial v}{\partial r} \mathbf{r} \cdot \nabla + \frac{1}{4} \nabla^2 v \right] \\ &\quad + \frac{1}{m_1 m_2} \left[v \frac{\partial^2}{\partial t^2} + \frac{\partial v}{\partial t} \frac{\partial}{\partial t} + \frac{1}{4} \frac{\partial^2 v}{\partial t^2} \right], \end{aligned} \quad (3.19b)$$

$$U_{SO} = \frac{h_M}{m_1 m_2} \left[\frac{1}{r} \frac{\partial v}{\partial r} \right] \mathbf{L} \cdot \mathbf{S}, \quad (3.19c)$$

$$U_T = \frac{h_M^2}{12m_1 m_2} \left[\frac{1}{r} \frac{\partial v}{\partial r} - \frac{\partial^2 v}{\partial r^2} \right] S_{12}, \quad (3.19d)$$

$$U_{SS} = \frac{h_M^2}{6m_1 m_2} (\nabla^2 v) \boldsymbol{\sigma}_1 \cdot \boldsymbol{\sigma}_2 \quad (3.19e)$$

with

$$v(x) = f_c \frac{\alpha_s}{2Fr} [\delta(r-t) + \delta(r+t)], \quad (3.20)$$

and

$$\mathbf{L} = \mathbf{L}_1 + \mathbf{L}_2, \quad \mathbf{L}_i = \mathbf{r}_i \times \mathbf{p}_i, \quad \mathbf{S} = \mathbf{S}_1 + \mathbf{S}_2,$$

$$\mathbf{S}_i = \frac{1}{2} \boldsymbol{\sigma}_i, \quad S_{12} = 3 \frac{\boldsymbol{\sigma}_1 \mathbf{r} \boldsymbol{\sigma}_2 \cdot \mathbf{r}}{r^2} - \boldsymbol{\sigma}_1 \cdot \boldsymbol{\sigma}_2.$$

The Coulomb-type and orbit-orbit-like interactions, U_C and U_{OO} , come from U_{GE} , the spin-orbit one U_{SO} from U_{GEM} , and the tensor and spin-spin ones, U_T and U_{SS} , from U_{GM} .

These expressions for the OGE potential have quite

similar forms to the standard Breit-Fermi Hamiltonian. In particular, if we take, neglecting the retardation effect, $v(r) = f_c \alpha_s / r$ and substitute $m_1 + m_2$ for M_0 and M'_0 in U_C , then we have the usual Coulomb potential. Furthermore, if we neglect the terms concerning the relative time in U_{OO} and take $h_M = 1$ in U_{SO} , U_T and U_{SS} , they become identical with the corresponding part due to the contribution of transverse gluons ($\gamma_i^{(1)} \otimes \gamma_i^{(2)}$ part) in the Breit-Fermi Hamiltonian in the Feynman gauge. The reason why the part due to the contribution of longitudinal gluons ($\gamma_4^{(1)} \otimes \gamma_4^{(2)}$ part) is missing, except for the U_C , in our scheme is that the small component of our spin wave function vanishes in the meson rest frame, as was mentioned above. [This part may be important, giving, for example, the spin-orbit interaction $\mathbf{L} \cdot (\mathbf{S}_1 - \mathbf{S}_2)$, which causes the mixing between the states ${}^3L_J \leftrightarrow {}^1L_J$ for non-self-conjugate mesons.]

Here it is worthwhile to note that, although our OGE potential has several similar general features, as mentioned above, to those in the usual NR potential models, there are essential differences between them; our scheme is manifestly covariant and our potential is concerned with the squared masses of mesons instead of with linear masses.

C. Effective three-dimensional OGE potential

In the meson rest frame the unperturbed internal wave function Ψ in Eq. (3.14), satisfying the subsidiary condition of Eq. (2.7), takes the form

$$\Psi(x) = \left[\frac{\beta}{\pi} \right]^{1/4} e^{-\beta t^2/2} \psi(\mathbf{r}) \phi_{\text{SF}}, \quad (3.21)$$

where $\beta = \sqrt{\mu K}$, $\psi(\mathbf{r})$ is the eigenfunction of the three-dimensional harmonic oscillator and ϕ_{SF} is the spin-flavor wave function, both of which are identical with the corresponding wave functions in the NR harmonic-oscillator quark model. Then the first-order squared-mass shifts due to the OGE potential are given by

$$\delta M_G^2(f|i) = d \int d^4x \Psi^{(\lambda')\dagger} U_G \Psi^{(\lambda)}, \quad (3.22)$$

where λ and λ' represent the sets of quantum numbers for specifying the initial and final states, respectively.

By using the expressions for U_G and v in Eqs. (3.19a)–(3.19e) and (3.20), respectively, and working out the integral over the relative time in Eq. (3.22), we obtain

$$\delta M_G^2(f|i) = d \int d^3\mathbf{r} \psi^{(\lambda')\dagger} \phi_{\text{SF}}^{(\lambda')\dagger} V_G \phi_{\text{SF}}^{(\lambda)} \psi^{(\lambda)}, \quad (3.23)$$

where

$$V_G = V_C + V_{OO} + V_{SO} + V_T + V_{SS} \quad (3.24)$$

with

$$V_C = -\frac{\alpha_s(M_0^{(N)} + M_0^{(N')})^2}{3(m_1 + m_2)^2} \left[\frac{\beta}{\pi F^2} \right]^{1/2} \frac{e^{-\beta r^2}}{r}, \quad (3.25a)$$

$$V_{OO} = -\frac{4\alpha_s}{3m_1 m_2} \left[\frac{\beta}{\pi F^2} \right]^{1/2} \frac{e^{-\beta r^2}}{r} \times \left[\left[\frac{1}{r^2} + 2\beta \right] \mathbf{r} \cdot \nabla - \nabla^2 + \pi r \delta^3(\mathbf{r}) - \beta^2 r^2 \right], \quad (3.25b)$$

$$V_{SO} = \frac{4\alpha_s h_M}{3m_1 m_2} \left[\frac{\beta}{\pi F^2} \right]^{1/2} \left[\frac{1}{r^3} + \frac{2\beta}{r} \right] e^{-\beta r^2} \mathbf{L} \cdot \mathbf{S}, \quad (3.25c)$$

$$V_T = \frac{\alpha_s h_M^2}{3m_1 m_2} \left[\frac{\beta}{\pi F^2} \right]^{1/2} \left[\frac{1}{r^3} + \frac{4\beta}{3r} + \frac{4}{3}\beta^2 r \right] e^{-\beta r^2} S_{12}, \quad (3.25d)$$

$$V_{SS} = \frac{2\alpha_s h_M^2}{9m_1 m_2} \left[\frac{\beta}{\pi F^2} \right]^{1/2} \times \left[4\pi \delta^3(\mathbf{r}) + \frac{2\beta}{r} - 4\beta^2 r \right] e^{-\beta r^2} \boldsymbol{\sigma}_1 \cdot \boldsymbol{\sigma}_2. \quad (3.25e)$$

Here α_s and F were assumed to be independent of the spatial and time separations, r and t , for simplicity. In these expressions the factor $\sqrt{\beta/\pi} e^{-\beta r^2}$ for each term of V_G comes from the relative-time wave function, and all the terms containing β result from the retardation effect (the factor $\frac{1}{2}[\delta(r-t) + \delta(r+t)]$ in v). We note here that the explicit potential forms from this effect completely depend on the relative-time wave function.

Thus we see that so far as the mass shifts are concerned, our model formally corresponds to the NR harmonic-oscillator quark model with replacement

$$V_G \text{ for } \delta M_G \rightarrow dV_G \text{ for } \delta M_G^2. \quad (3.26)$$

Moreover, our three-dimensionally reduced potential V_G is greatly modified as compared with the usual one. The modification of multiplying the factor $e^{-\beta r^2}$ causes our effective potential to decrease more quickly with the increase of a quark-antiquark separation. The extra terms due to the retardation effect generally contribute comparably to the usual ones. The Coulomb-type potential V_C is dependent upon the unperturbed masses of the relevant states. The quark-mass dependence of mass shifts will change, reflecting the quark-mass dependence of β , F , and d . These modifications play important roles to reproduce the experimental behavior of meson spectra, as we shall see later.

IV. COMPARISON WITH EXPERIMENT

According to the results in the previous sections the squared masses of respective mesons for all the states of given quark content are given as

$$M^2 = (M_0^{(N)})^2 + \delta M_G^2. \quad (4.1)$$

The unperturbed squared mass $(M_0^{(N)})^2$ is described by the parameters $(M_0^{(0)})^2$ and Ω [see Eq. (3.4)]. The first-order squared-mass shift due to the OGE effects δM_G^2 is given as the sum of

$$\delta M_G^2 = \delta M_C^2 + \delta M_{OO}^2 + \delta M_{SO}^2 + \delta M_T^2 + \delta M_{SS}^2, \quad (4.2)$$

where δM_C^2 , δM_{OO}^2 , δM_{SO}^2 , δM_T^2 , and δM_{SS}^2 are the Coulomb-type, orbit-orbit-like, spin-orbit, tensor, and spin-spin mass shifts and are represented, respectively, by $((M_0^{(0)})^2, \Delta, \Omega)$, Δ , $h_M \Delta$, $h_M^2 \Delta$, and $h_M^2 \Delta$ (the explicit formulas of $\delta M_i^2 \equiv d\langle U_i \rangle$ for the relevant states are given in Appendix B).

Thus the mass spectrum of the mesons with given quark content is described by the four parameters

$$(M_0^{(0)})^2, \Omega, h_M, \Delta \equiv d\delta = \frac{16\alpha_s K}{9\pi F}. \quad (4.3)$$

All of these parameters may, in principle, depend on the constituent-quark masses of mesons.

A. Universality of Regge slopes and spin-spin splittings, and fixing parameters

Experimentally it is well known that the linearity of the leading Regge trajectories is extremely well satisfied, and their slopes, given by Ω^{-1} , have the universal value as

$$\Omega(n\bar{n}) \simeq \Omega(n\bar{s} \text{ or } s\bar{n}) \simeq \Omega(s\bar{s}) \simeq 1.15 \text{ GeV}^2 \quad (4.4)$$

regardless of the quark contents of mesons. In Figs. 1–4 we have shown the Regge trajectories of ρ , ω , \bar{K}^* , and ϕ mesons, respectively. As was mentioned in the previous sections, in our scheme this linearity is rigorously satisfied in the unperturbed limit and will be shown to change little even in the perturbed case (see the discussion in Sec. V C). Thus we take the parameter Ω to be a flavor-independent constant with the value given in Eq. (4.4). From Eq.

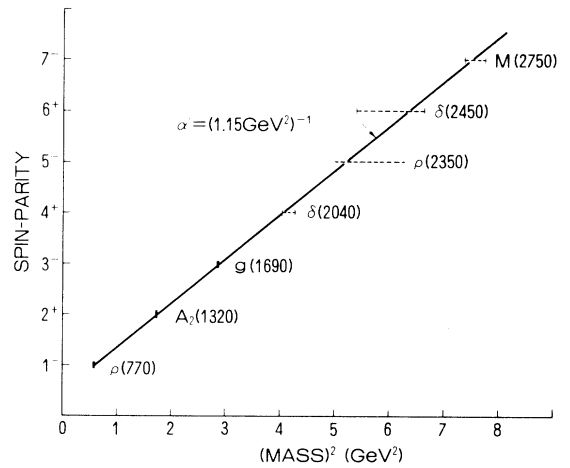


FIG. 1. The ρ -meson trajectory. The straight line shows our theoretical Regge trajectory in the unperturbed limit with the values of the parameters fixed in the text. The solid (dashed) bars represent the experimental masses of established (not established) resonances, and their values are taken from Ref. 17 except for $M(2750)$ from Ref. 22.

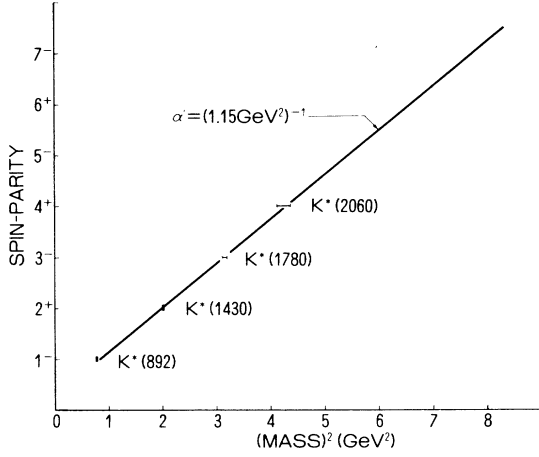


FIG. 2. The K^* -meson trajectory. The caption is the same as in Fig. 1.

(3.5b) this implies that the oscillator constant K in Eq. (3.3) has the quark-mass dependence

$$K = \frac{m_1 m_2}{4(m_1 + m_2)^3} \Omega^2. \quad (4.5)$$

Also known is the empirical regularity that the spin-spin splittings of ground-state mesons $M^2(1^3S_1) - M^2(1^1S_0)$ are nearly a flavor-independent constant, at least for the light-quark mesons as is shown in Table I.

Thus, from the formula

$$M^2(1^3S_1) - M^2(1^1S_0) = 4h_M^2 \Delta \quad (4.6)$$

and the value of

$$M^2[\rho] - M^2[\pi] \simeq M^2[K^*] - M^2[K] \simeq 0.563 \text{ GeV}^2, \quad (4.7)$$

we fix the parameter $h_M^2 \Delta$ to be a flavor-independent constant of the value 0.141 GeV^2 . In the following we simply assume h_M and Δ to be separately flavor indepen-

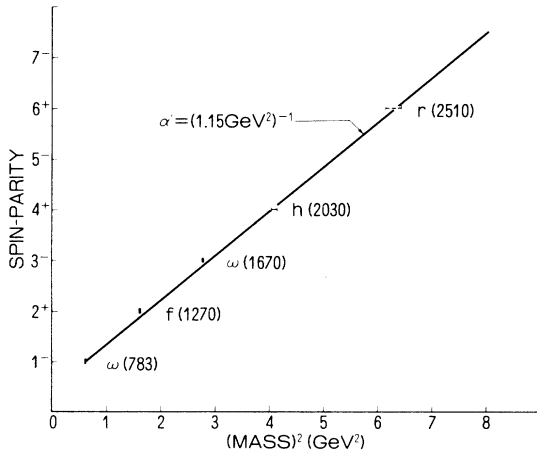


FIG. 3. The ω -meson trajectory. The caption is the same as in Fig. 1. The line represents the trajectory for pure $n\bar{n}$ systems.

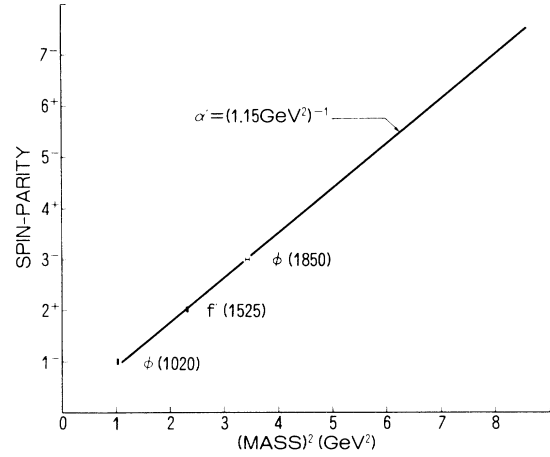


FIG. 4. The ϕ -meson trajectory. The caption is the same as in Fig. 1. The line represents the trajectory for pure $s\bar{s}$ systems.

dent. The constancy of Δ implies²⁰ from Eq. (4.3), neglecting the flavor dependence of α_s , that F has the same quark-mass dependence as K :

$$F = \frac{m_1 m_2}{4(m_1 + m_2)^3} \Lambda, \quad (4.8)$$

where Λ is the flavor-independent constant with the dimension of $(\text{mass})^2$.

According to the above considerations, all the meson mass spectra of the light-quark systems are described by the six parameters Ω , h_M , Δ , $(M_0^{(0)})^2(n\bar{n})$, $(M_0^{(0)})^2(n\bar{s} \text{ or } s\bar{n})$, and $(M_0^{(0)})^2(s\bar{s})$. We have already fixed two (Ω and $h_M^2 \Delta$) of them. As input to determine the remaining four parameters we take the mass values

$$\begin{aligned} M(1^1S_0; n\bar{n}) &= M[\pi] \simeq 140 \text{ MeV}, \\ M(2^3S_1; n\bar{n}) &= M[\rho(1600)] \simeq 1600 \text{ MeV}, \\ M(1^1S_0; n\bar{s} \text{ or } s\bar{n}) &= M[K] \simeq 494 \text{ MeV}, \\ M(1^3S_1; s\bar{s}) &= M[\phi(1020)] \simeq 1020 \text{ MeV}. \end{aligned} \quad (4.9)$$

This gives our parameters the values

$$\begin{aligned} \Delta &\simeq 0.0493 \text{ GeV}^2 \quad (h_M \simeq 1.69), \\ (M_0^{(0)})^2(n\bar{n}) &\simeq 0.592 \text{ GeV}^2, \\ (M_0^{(0)})^2(n\bar{s} \text{ or } s\bar{n}) &\simeq 0.849 \text{ GeV}^2, \\ (M_0^{(0)})^2(s\bar{s}) &\simeq 1.116 \text{ GeV}^2, \end{aligned} \quad (4.10)$$

where we have chosen positive sign of h_M in order to give the favorable fine structures to the orbitally excited multiplets.

Now, using these values of parameters, we can calculate the masses of all light-quark mesons. In the following we shall concentrate our investigation on the ‘‘center of gravity’’ of the respective multiplets, the spectra of S -wave mesons and of several orbitally excited-state mesons.

TABLE I. The universality of spin-spin splittings of the ground-state mesons with various quark content.

Flavor composition	$M^2(1^3S_1) - M^2(1^1S_0)$	Experiment ^a (GeV ²)
$n\bar{n}$ ($I=1$)	$\rho^2 - \pi^2$	0.5664–0.5765
$n\bar{s}$ or $s\bar{n}$	$K^{*2} - K^2$	0.5514–0.5567
$n\bar{c}$ or $c\bar{n}$	$D^{*2} - D^2$	0.5408–0.5624
$s\bar{c}$ or $c\bar{s}$	$F^{*2} - F^2$	0.491–0.647 ^b
$n\bar{b}$ or $b\bar{n}$	$B^{*2} - B^2$	0.4789–0.6381 ^c
$c\bar{c}$	$J/\psi^2 - \eta_c^2$	0.6680–0.7408

^aFrom Ref. 17, unless otherwise noted.

^bReference 18.

^cReference 19.

B. Center of gravity of multiplets and general feature of our fitting

To see general features of our scheme in comparison with experiment we first examine for all the meson states the center of gravity (COG), or the spin-weighted average, of the respective multiplets with a definite value of the principal quantum number $N (=2n+L-2)$ and of the orbital angular momentum L , which is concerned only with the confinement potential, and the Coulomb-type and orbit-orbit-like interactions:

$$\bar{M}^2(n, L) = (M_0^{(N)})^2 + \delta M_C^2 + \delta M_{OO}^2. \quad (4.11)$$

We have given the calculated values of M_0^2 , δM_C^2 , δM_{OO}^2 , and \bar{M} of the multiplets with $N \leq 6$ for the $n\bar{n}$, $n\bar{s}$ or $s\bar{n}$, and $s\bar{c}$ systems, respectively, in Tables II–IV, where the experimental candidates belonging to the respective multiplets are also given for comparison. An overall view of the status of our fit may be obtained from the corresponding figures, Figs. 5–8, to these tables. In Tables II and IV (correspondingly Figs. 7 and 8) we have simply neglected the possible flavor mixings of the isoscalar mesons. Furthermore, we have omitted the experimental candidates for scalar mesons from these tables and figures, because their interpretation is controversial.

By inspecting the tables and figures given above we see that our scheme reproduces the general feature of the meson spectra.

C. S-wave states and spin-spin splittings

To compare more clearly our predictions with experiments we examine the S-wave states. Their masses are determined from the confinement potential and Coulomb-type, orbit-orbit-like, and spin-spin interactions, neglecting the possible mixing between the 3S_1 and 3D_1 states due to the tensor interaction, as

$$M^2(n^{2S+1}L_J) = (M_0^{(N)})^2 + \delta M_C^2 + \delta M_{OO}^2 + \delta M_{SS}^2 \quad (4.12)$$

($N=2n-2$). We have given the calculated values of mass M and δM_{SS}^2 of these states with $N \leq 6$ for each $q\bar{q}$ system, together with the present experimental mass values in Table V. The values of M_0^2 , δM_C^2 , and δM_{OO}^2 were already given in Tables II–IV. The situations are also shown in Figs. 9–11.

From these tables and figures we may say that our scheme is satisfactory as far as the present experiments, even though poor, are concerned.

D. Several orbitally excited states, and fine and hyperfine splittings

We now turn to the investigation of the fine and hyperfine structures of orbitally excited multiplets. These structures are determined by the spin-orbit, tensor, and spin-spin interactions. The mass of the states belonging to these multiplets is given by

$$M^2(n^{2S+1}L_J) = (M_0^{(N)})^2 + \delta M_C^2 + \delta M_{OO}^2 + \delta M_{SO}^2 + \delta M_T^2 + \delta M_{SS}^2, \quad (4.13)$$

where we have neglected the possible mixing due to the tensor interaction. Here it is to be noted that in our scheme the “asymmetric” spin-orbit interaction, which is responsible for the mixing between non-self-conjugate mesons, is missing, as was mentioned in Sec. III B. On the other hand, it is to be noted that in our scheme the contribution of the spin-spin interaction exists for orbitally excited states, reflecting the retardation effect. We have given the calculated value of the mass M , δM_{SO}^2 , δM_T^2 , and δM_{SS}^2 for the states of $1P$, $1D$, $2P$, $1F$, $2D$, and $3P$ multiplets for each $q\bar{q}$ system, together with the mass value of the present experimental candidates, in Table VI.

We find that the predicted mass of 3P_0 states is much lower than that of other members of the same multiplets. Although the interpretation of the known scalar-meson resonances is controversial, it is interesting that our predicted mass of the scalar meson with $n\bar{n}$ components is quite close to that of $\delta(980)$ and/or $S(975)$. From this table it seems that our predicted sign and order of magnitude of the spin-orbit and the tensor interactions are consistent so far as the present experimental data are concerned.

V. SOME SPECIFIC FEATURES OF OUR SCHEME

In this section we discuss some specific features to our scheme.

TABLE II. The centers of gravity of the $n\bar{n}$ -meson multiplets. The unperturbed squared masses and the Coulomb-type and orbit-orbit-like squared-mass shifts are also given. The experimental candidates of the isovector mesons and the isoscalar ones (with mainly $n\bar{n}$ components) are listed on the upper and lower sides, respectively.

Level	M_0^2 (GeV ²)	δM_C^2 (GeV ²)	δM_{OO}^2 (GeV ²)	\bar{M} (MeV)	Experiment ^a (MeV)			
					¹ L_L	³ L_{L-1}	³ L_L	³ L_{L+1}
1S	0.592	−0.076	−0.074	665	π	$\rho(770)$
					137.3±2.3	769±3
					η^b	$\omega(783)$
					548.8±0.6			782.6±0.2
1P	1.742	−0.075	−0.099	1250	$B(1235)$		$A(1270)$	$A_2(1320)$
					1234±10		1275±30	1318±5
					$H(1190)$		$D(1285)$	$f(1270)$
					1190±60		1283±5	1274±5
2S	2.892	−0.310	−0.259	1520	$\pi(1300)$	$\rho(1600)$
					1300±100	1590±20
					$\eta(1275)$	
					~1275			
1D	2.892	−0.050	−0.059	1670	$A(1680)$			$g(1690)$
					1680±30			1691±5
								$\omega(1670)$
								1668±5
2P	4.042	−0.190	−0.217	1910				
1F	4.042	−0.030	−0.034	1990			$A(2050)$	$\delta(2040)$
							2080±40	2037±5
								$h(2030)$
								2027±12
3S	5.192	−0.495	−0.410	2070	$\pi(1770)$	$\rho(2150)$
					1770±30	~2150
						
2D	5.192	−0.121	−0.134	2220	$A(2100)$			$\rho(2250)$
					2100±150			~2250
1G	5.192	−0.017	−0.019	2270				$\rho(2350)^c$
								~2350
3P	6.342	−0.300	−0.326	2390				
2F	6.342	−0.075	−0.082	2490				
1H	6.342	−0.009	−0.010	2510				$\delta(2450)$
								2450±130
								$r(2510)$
								2150±30
4S	7.492	−0.655	−1.202	2370		
						
1I	7.492	−0.005	−0.006	2740				$M(2750)^d$
								2747±32

^aThe experimental masses, which are taken from Ref. 17, unless otherwise noted, are shown under the respective particle names.

^bThis meson is a strongly mixed state of the $n\bar{n}$ and $s\bar{s}$ components.

^cThere is another candidate for the 1^3G_5 state; see Ref. 21.

^dReference 22.

TABLE III. The centers of gravity of the $n\bar{s}$ - or $s\bar{n}$ -meson multiplets. The unperturbed squared masses, the Coulomb-type and orbit-orbit-like squared-mass shifts, and the experimental candidates are also given.

Level	M_0^2 (GeV ²)	δM_C^2 (GeV ²)	δM_{OO}^2 (GeV ²)	\bar{M} (MeV)	Experiment ^a (MeV)			
					1L_L	$^3L_{L-1}$	3L_L	$^3L_{L+1}$
1S	0.849	-0.109	-0.074	816	K 495.7±2.1	K*(892) 894±3
1P	1.999	-0.086	-0.099	1350	Q(1400) ^b 1406±10		Q(1280) ^b 1270±10	K*(1430) 1425±5
2S	3.149	-0.337	-0.259	1600	K(1400) ~1400	K*(1650) ~1650
1D	3.149	-0.054	-0.059	1740	L(1770) ^c ~1770	K*(1790) ^d 1786±12	L(1580) ^c ~1580	K*(1780) 1780±10
2P	4.299	-0.203	-0.217	1970				
1F	4.299	-0.032	-0.034	2060				K*(2060) 2060±30
3S	5.449	-0.519	-0.410	2130	K(1830) ~1830	
2D	5.449	-0.127	-0.134	2280			K(2250) ^c 2247±18	
1G	5.449	-0.018	-0.019	2330				
3P	6.599	-0.312	-0.326	2440				
2F	6.599	-0.078	-0.082	2540			K(2320) ^c 2324±25	
1H	6.599	-0.010	-0.010	2560				
4S	7.749	-0.678	-1.202	2420		
1I	7.749	-0.005	-0.006	2780				

^aSee footnote a of Table II.

^bThese mesons are mixtures of the 1P_1 and 3P_1 states.

^cThese mesons are possibly mixtures of the 1D_2 and 3D_2 states.

^dReference 23.

^eThis meson is possibly a mixture of the 1F_3 and 3F_3 states.

A. Spin-spin splittings

We have already discussed in Sec. IV A that the remarkable experimental regularity of flavor-independent spin-spin splittings of the ground-state mesons is incorporated naturally in our scheme. We can derive another interesting flavor-independent sum rule between the spin-spin splittings of the ground states and their first radially excited states as

$$R \equiv \frac{M^2(2^3S_1) - M^2(2^1S_0)}{M^2(1^3S_1) - M^2(1^1S_0)} = \frac{5}{3}, \quad (5.1)$$

which is related mainly with the nature of unperturbed oscillator functions at the origin. Our spin-spin potential

consists of the two parts of the pointlike interaction and the interaction due to the retardation effect [see Eq. (3.25e)]. If we neglected the latter, the second and third term in Eq. (3.25e), the ratio R would become equal to $\frac{3}{2}$, and the retardation part gives a positive contribution with the size of about 10% relative to the pointlike one. Experimentally we know the ratios for the isovector and isodoublet mesons, respectively, as

$$R_1(n\bar{n}) = \frac{\rho^2(1600) - \pi^2(1300)}{\rho^2 - \pi^2} = 1.47^{+0.56}_{-0.59} (0.46 \pm 0.20), \quad (5.2)$$

$$R_{1/2}(n\bar{s} \text{ or } s\bar{n}) = \frac{K^{*2}(1650) - K^2(1400)}{K^{*2} - K^2} \sim 1.4 (\sim 0.63),$$

TABLE IV. The centers of gravity of the $s\bar{s}$ -meson multiplets. The unperturbed squared masses and the Coulomb-type and orbit-orbit-like mass shifts are also given. As for their experimental candidates the isoscalar mesons with mainly $s\bar{s}$ components are simply given.

Level	M_0^2 (GeV ²)	δM_C^2 (GeV ²)	δM_{OO}^2 (GeV ²)	\bar{M} (MeV)	Experiment ^a (MeV)			
					1L_L	$^3L_{L-1}$	3L_L	$^3L_{L+1}$
1S	1.116	-0.143	-0.074	948	$\eta'(958)^b$ 957.57±0.25	$\phi(1020)$ 1019.5±0.1
1P	2.266	-0.097	-0.099	1440			$E(1420)$ 1418±10	$f'(1525)$ 1525±5
2S	3.416	-0.366	-0.259	1670		$\phi(1680)$ 1685±10
1D	3.416	-0.059	-0.059	1820				$\phi(1850)$ 1853±10
2P	4.566	-0.215	-0.217	2030				
1F	4.566	-0.034	-0.034	2120				
3S	5.716	-0.545	-0.410	2180		
2D	5.716	-0.133	-0.134	2330				
1G	5.716	-0.019	-0.019	2380				
3P	6.866	-0.325	-0.326	2490				
2F	6.866	-0.081	-0.082	2590				
1H	6.866	-0.010	-0.010	2620				
4S	8.016	-0.701	-1.202	2470		
1I	8.016	-0.005	-0.006	2830				

^aSee footnote a of Table II.

^bSee footnote b of Table II.

which are close to our prediction. However, we need the further confirmation of the existence of $K(1400)$ and $K^*(1650)$ and of the $q\bar{q}$ assignments²⁵ for these resonances. In the case of the NR harmonic-oscillator quark model we derive a similar sum rule for linear masses, where the ratio R is equal to $\frac{3}{2}$ because of no retardation effect. However, in this case the prediction seems to contradict the experimental values given in the respective parentheses of Eq. (5.2).

There is another interesting feature that our spin-spin potential contributes to the splittings of orbitally excited states due to the retardation effect. This contribution is positive and negative for spin-singlet and spin-triplet states, respectively, in contrast with the case of S -wave states. Its size is as small as a few percent or less of the unperturbed squared masses, as is seen from Table VI,

and does not affect the general feature of the mass spectra.

B. Coulomb-type and orbit-orbit-like splittings

As was mentioned in Sec. III C, our Coulomb-type potential is greatly modified, as compared with the usual one, in addition to the fact that our potentials are concerned directly with the squared masses. From Tables II–IV we find that the Coulomb-type and orbit-orbit-like squared-mass shifts are roughly of the same size. From these tables and Figs. 5–8 we also see that these spin-independent squared-mass shifts for the pure orbitally excited states are quite small (in practice negligible for the states with $L \geq 3$), while they give considerable contributions for the radially excited S -wave states. These features seem to be supported experimentally.

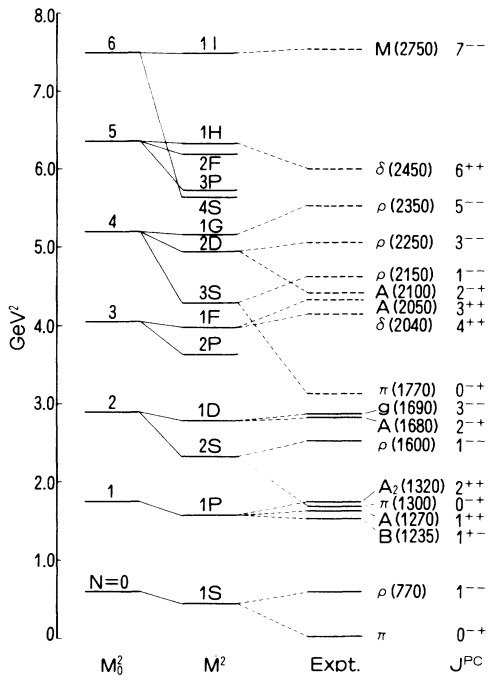


FIG. 5. The centers of gravity of the multiplets for isovector ($n\bar{n}$) mesons in comparison with experiment. In the third column the established (not established) resonances are shown by solid (dashed) lines.

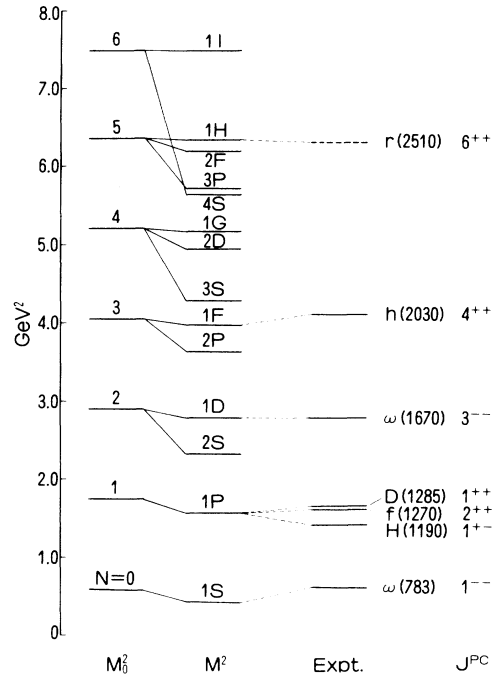


FIG. 7. Same as in Fig. 5, for isoscalar ($n\bar{n}$) mesons.

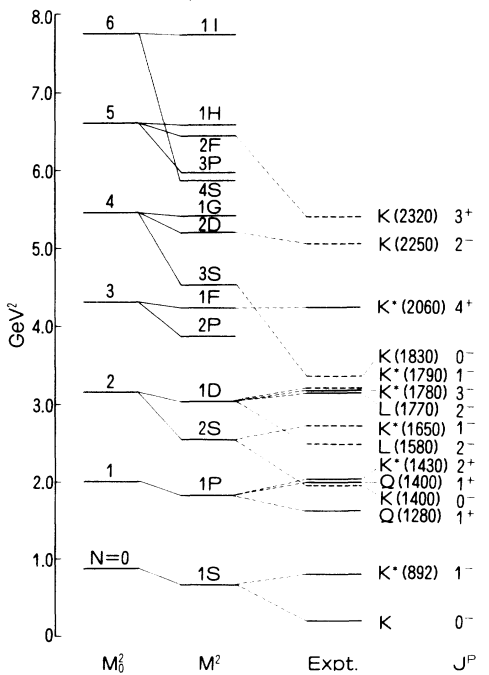


FIG. 6. Same as in Fig. 5, for isodoublet ($n\bar{s}$ or $s\bar{n}$) mesons.

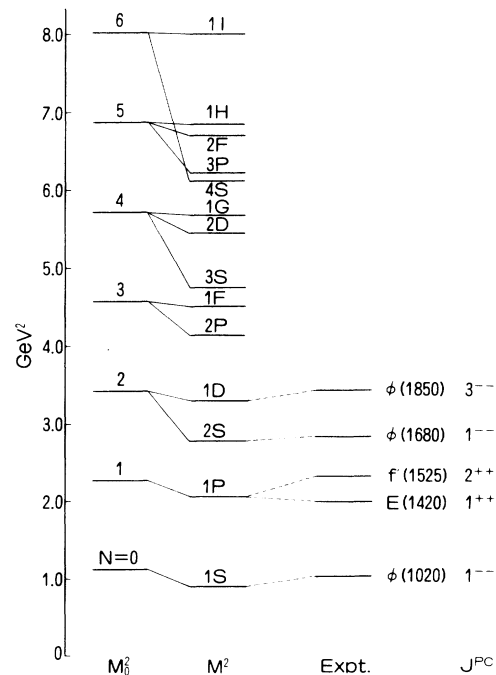


FIG. 8. Same as in Fig. 5, for isoscalar ($s\bar{s}$) mesons.

TABLE V. The S -wave mesons. The masses and the spin-spin squared-mass shifts for the isovector ($n\bar{n}$), isodoublet ($n\bar{s}$ or $s\bar{n}$), and isoscalar ($s\bar{s}$) mesons are given. The experimental masses are also given in parentheses and the input values are underlined.

State	δM_{ss}^2 (GeV ²)	Mass (MeV)		
		$n\bar{n}$ ($I=1$)	$n\bar{s}$ or $s\bar{n}$	$s\bar{s}$
1^1S_0	-0.422	<u>140</u>	494	690 (...)
1^3S_1	0.141	763 (769±3)	898 (894±3)	<u>1020</u>
2^1S_0	-0.704	1270 (1300±100)	1360 (~1400)	1440
2^3S_1	0.235	<u>1600</u>	1670 (~1650)	1740 (1685±10)
3^1S_0	-0.869	1850 (1770±30)	1910 (~1830)	1970
3^3S_1	0.290	2140 (~2150)	2190	2250
4^1S_0	-1.001	2150	2210	2260
4^3S_1	0.334	2440	2490	2540

In order to see the validity of our Coulomb-type and orbit-orbit-like potentials, the orbitally excited ($L \neq 0$) isovector ($I=1$) spin-singlet ($S=0$) states are especially interesting, since their mass shifts are almost given by these potentials (the contribution from the spin-spin potential is small, as mentioned above) and there are no possibilities of the spin-orbit and flavor mixings. At present we have the three experimental candidates for these states:

$B(1235)$, $A(1680)$, and $A(2100)$ to be assigned to ($n^{2S+1}L_J =$) 1^1P_1 , 1^1D_2 , and 2^1D_2 , respectively, whose experimental mass values seem to be close to our predictions (see Table VI).

C. Spin-orbit and tensor splittings

Our spin-orbit and tensor squared-mass shifts, which are described by the parameters $h_M \Delta$ and $h_M^2 \Delta$, respec-

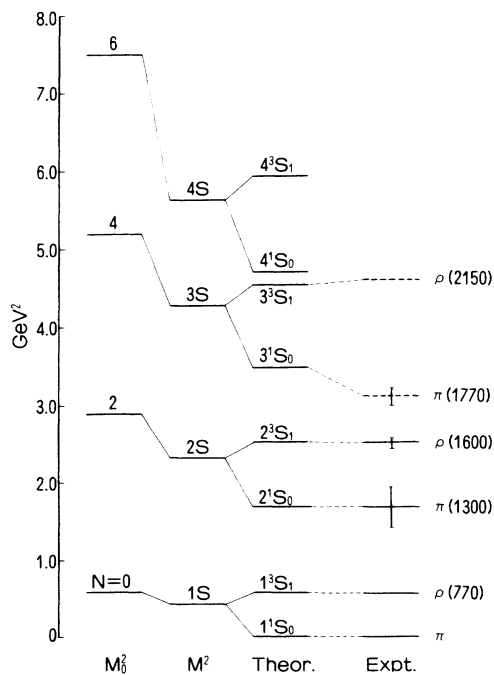


FIG. 9. The mass spectrum of the isovector ($n\bar{n}$) S -wave mesons in comparison with experiment.

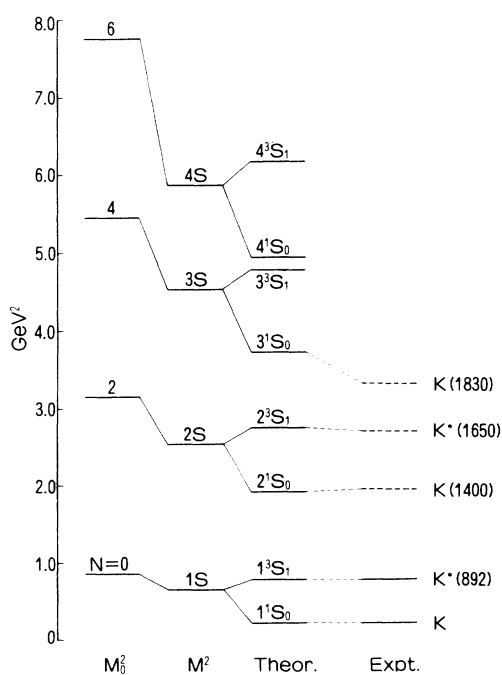


FIG. 10. The mass spectrum of the isodoublet ($n\bar{s}$ or $s\bar{n}$) S -wave mesons in comparison with experiment.

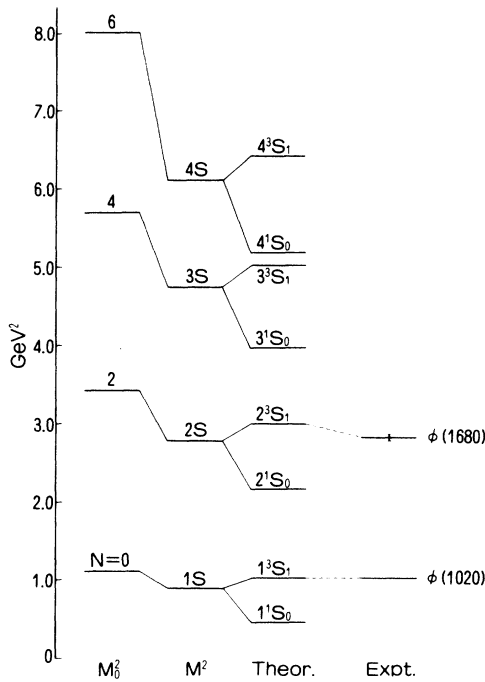


FIG. 11. The mass spectrum of the isoscalar ($s\bar{s}$) S -wave mesons in comparison with experiment.

tively, also become flavor independent, corresponding to the flavor independence of the spin-spin splittings. To our regret, we cannot check its validity presently, since the experimental knowledge is poor.

We also note that our spin-dependent potentials contain the effect of a color-anomalous moment interaction ($h_M = 1.69 \neq 1$), in contrast with the case in the standard NR potential models ($h_M = 1$). Therefore, the strength of the tensor interaction becomes the larger relative to the spin-orbit one. (It is to be noted that the above value of the color-anomalous moment was determined only from the analysis of the S -wave mesons.) In our analysis a color-anomalous interaction seems to play an important role in reproducing the consistent fine and hyperfine structures.

Furthermore, we remark that our spin-orbit [Eq. (3.25c)] and tensor potentials [Eq. (3.25d)] contain the extra term due to the retardation effect, as in the case of the spin-spin one. This contribution is about as large as that of the usual term.

The magnitude of the spin-orbit and tensor squared-mass shifts is comparable only for the lower- L states and becomes as small as a few percent or less of the unperturbed square masses for the states with $L \geq 3$, as is seen from Table VI.

D. Linearity of leading Regge trajectories

Reproducing the experimental fact (the linearity of leading Regge trajectories) in the unperturbed limit was

one of the most important features of the COQM. The remarkable regularity of universal Regge slopes for all the meson systems was also incorporated in our scheme in the unperturbed limit.

We can now see the OGE effects on the leading Regge trajectories from Tables II–VI. We find that the total squared-mass shifts are about 4% of the unperturbed masses even for 1^3P_2 states, to which they give the largest contribution. We note here that for 1^3S_1 and 1^3P_2 states the spin-independent (Coulomb-type and orbit-orbit-like) and the spin-dependent (spin-orbit, tensor, and spin-spin) contributions are individually sizable, but they mostly cancel out each other. Therefore, the linearity of the leading Regge trajectories is preserved in the perturbed case.

VI. CONCLUDING REMARKS

In this paper we have extended the COQM so as to include the OGE effects covariantly and applied it to investigate the light-quark meson spectra. The effects are included as a first-order perturbation in our specific scheme. Our OGE potential consists of Coulomb-type, orbit-orbit-like, spin-orbit, and hyperfine interactions, and each of them formally corresponds to the respective parts due to the contribution of transverse gluons in the Breit-Fermi Hamiltonian in the Feynman gauge. However, these potentials are modified, because of their covariant nature, as follows. First, all of them contain the retardation effect. Second, the Coulomb-type potential depends on the unperturbed masses of relevant mesons in the meson rest frame. Third, the orbit-orbit-like potential has the contribution of the motion concerning the relative-time freedom. It should also be noted that our potentials are concerned directly with the squared mass of mesons.

The centers of gravity for most of the multiplets with the number of oscillator quanta $N \leq 6$ and the spectra of excited S -wave mesons and of several orbitally excited ones were calculated, simply neglecting the mixing of $^3L_J \leftrightarrow ^3L'_J$, $^1L_J \leftrightarrow ^3L_J$ and of flavor, and compared with experiment. As a result, we may conclude that our scheme reproduces consistently the experimental behavior of the light-quark meson spectra. One of the most important features of the COQM is to reproduce the linearity of leading Regge trajectories in the unperturbed limit. We have examined the OGE effects on the leading trajectories and found that they affected little the linearity of them.

Our Coulomb-type and orbit-orbit-like potentials induce the mass reduction of a fair amount for the radially excited S -wave states, while they affect only a little the pure orbitally excited states, in conformity with experimental behavior. The spin-spin potential also seems to be satisfactory. We withhold a definite conclusion for our spin-orbit and tensor potentials, since the experimental knowledge is poor. However, it is to be noted that our spin-orbit potential lacks the part corresponding to the contribution of longitudinal gluons, and furthermore we may need the spin-orbit interaction due to an effective scalar exchange, as in the standard models.

We now turn to mentioning some defects in our

TABLE VI. The orbitally excited state mesons. The masses and the spin-orbit, tensor, and spin-spin squared-mass shifts for the isovector ($n\bar{n}$), isodoublet ($n\bar{s}$ or $s\bar{n}$), and isoscalar ($s\bar{s}$) mesons are given. The experimental masses are also given in parentheses.

State	δM_{SO}^2 (GeV ²)	δM_{T}^2 (GeV ²)	δM_{SS}^2 (GeV ²)	Mass (MeV)		
				$n\bar{n}$ ($I=1$)	$n\bar{s}$ or $s\bar{n}$	$s\bar{s}$
1^1P_1	0	0	0.070	1280 (1234±10)	1370 (1370±20) ^a	1460
1^3P_0	-0.333	-0.328	-0.023	940	1060	1180
1^3P_1	-0.167	0.164	-0.023	1240 (1275±30)	1340 (1310±15) ^a	1430 (1418±10)
1^3P_2	0.167	-0.033	-0.023	1300 (1318±5)	1390 (1425±5)	1480 (1525±5)
1^1D_2	0	0	0.056	1690 (1680±30)	1760	1830
1^3D_1	-0.150	-0.061	-0.019	1600	1680 (1786±12)	1750
1^3D_2	-0.050	0.061	-0.019	1670	1740	1810
1^3D_3	0.100	-0.017	-0.019	1690 (1691±5)	1760 (1780±10)	1830 (1853±10)
2^1P_1	0	0	0.021	1910	1980	2040
2^3P_0	-0.466	-0.408	-0.007	1660	1730	1800
2^3P_1	-0.233	0.204	-0.007	1900	1960	2020
2^3P_2	0.233	-0.041	-0.007	1950	2020	2080
1^1F_3	0	0	0.036	2000	2070	2130
1^3F_2	-0.076	-0.023	-0.012	1970	2030	2090
1^3F_3	-0.019	0.028	-0.012	1990 (2080±40)	2060	2120
1^3F_4	0.057	-0.009	-0.012	2000 (2037±27)	2070 (2060±30)	2130
2^1D_2	0	0	0.040	2230 (2100±150)	2290	2340
2^3D_1	-0.232	-0.079	-0.013	2150	2210	2260
2^3D_2	-0.077	0.079	-0.013	2220	2280	2330
2^3D_3	0.155	-0.022	-0.013	2250 (~2250)	2300	2360
3^1P_1	0	0	0.001	2390	2440	2490
3^3P_0	-0.560	-0.474	~0	2160	2220	2280
3^3P_1	-0.280	0.237	~0	2380	2430	2480
3^3P_2	0.280	-0.047	~0	2440	2490	2540

^aThese mass values are taken from Ref. 24.

scheme. One such vital defect is that the space-time part and the spin one of the unperturbed wave function are decoupled from each other, since they are covariantly generalized, separately, and the coupling between the two parts in the gluon vertices has been switched on by hands. This is a reason which has led us to vanishing of the “small components”²⁶ of our spin wave function in the hadron rest frame and accordingly to missing of the interaction corresponding to a longitudinal gluon exchange (except for a Coulomb-type interaction). Second, we cannot apply the present scheme directly to heavy-quark systems, where the perturbative treatment of the Coulomb-type potential may not be permissible. Apart from such rather technical problems there remain fundamental questions of how our scheme is related to the standard treatments such as the Bethe-Salpeter equation²⁷ and to the linear confinement model motivated by QCD. The latter question is under investigation.

Finally we should like to refer to the recent attempt²⁸

closely related to ours, which investigated light- and heavy-quark meson spectra in a unified and covariant way. This approach starts from the mutually consistent two coupled covariant wave equations for $q\bar{q}$ systems. This avoids the introduction of redundant relative-time freedom from the beginning, while it seems to make very complex a covariant description of the center-of-mass motion of hadrons.

ACKNOWLEDGMENTS

We should like to express our deep gratitude to Dr. M. Oda and N. Honzawa for their useful discussions and cooperation in our related works.

APPENDIX A: UNPERTURBED WAVE FUNCTIONS

The internal meson wave functions for the states with the definite radial quantum number N' , orbital angular

momentum L , total quark spin S , and total angular momentum J and its third component M are, in the meson rest frame, given by

$$\Psi_{NLS}^{JM}(x) = \left[\frac{\beta}{\pi} \right]^{1/4} e^{-\beta r^2/2} \psi_{NLS}^{JM}(\mathbf{r}), \quad (\text{A1})$$

where

$$\psi_{NLS}^{JM}(\mathbf{r}) = R_{N'L}(r) \mathcal{Y}_{LS}^{JM}(\theta, \phi) \quad (\text{A2})$$

includes the radial part

$$R_{N'L}(r) = N_{N'L} r^L e^{-\beta r^2/2} F(-N', L + \frac{3}{2}; \beta r^2) \quad (\text{A3})$$

with

$$|N_{N'L}| = \left[\frac{2^{-N'+L+2} (2N'+2L+1)!!}{N'! [(2L+1)!!]^2} \right]^{1/2} \left[\frac{\beta^{2L+3}}{\pi} \right]^{1/4} \quad (\text{A4})$$

and the confluent hypergeometric function

$$F(a, b; z) = \sum_{n=0}^{\infty} \frac{\Gamma(a+n)\Gamma(b)}{\Gamma(a)\Gamma(b+n)} \frac{z^n}{n!} \quad (\text{A5})$$

and the angular momentum part

$$\mathcal{Y}_{LS}^{JM}(\theta, \phi) = \sum_{m, \mu} Y_{Lm}(\theta, \phi) \chi_{S\mu} \langle LS m \mu | JM \rangle \quad (\text{A6})$$

with the usual spherical harmonics $Y_{Lm}(\theta, \phi)$ and the spin wave functions $\chi_{S\mu}$. In these formulas, the principal quantum number $N = 2N' + L$, $\beta = \sqrt{\mu} K$, and the flavor and color wave functions are omitted for simplicity.

APPENDIX B: DIAGONAL MATRIX ELEMENTS

The first-order squared-mass shifts are obtained by calculating the diagonal matrix elements of U_G as

$$\delta M_G^2(n^{2S+1}L_J) = d \langle n^{2S+1}L_J | U_G | n^{2S+1}L_J \rangle, \quad (\text{B1})$$

where $n = N' + 1$. Here we list some diagonal matrix elements used in the calculations of the text.

For the S -wave states, the Coulomb-type, orbit-orbit-like, and spin-spin potentials, U_C , U_{OO} , and U_{SS} , contribute to their matrix elements. They are given, up to the fourth S -wave states, by

bute to their matrix elements. They are given, up to the fourth S -wave states, by

$$\langle 1S | U_C | 1S \rangle = -3\delta\xi, \quad (\text{B2})$$

$$\langle 2S | U_C | 2S \rangle = -\frac{5}{2}\delta(\xi+2), \quad (\text{B3})$$

$$\langle 3S | U_C | 3S \rangle = -\frac{89}{40}\delta(\xi+4), \quad (\text{B4})$$

$$\langle 4S | U_C | 4S \rangle = -\frac{1143}{560}\delta(\xi+6), \quad (\text{B5})$$

$$\langle 1S | U_{OO} | 1S \rangle = -\frac{3}{2}\delta, \quad (\text{B6})$$

$$\langle 2S | U_{OO} | 2S \rangle = -\frac{21}{4}\delta, \quad (\text{B7})$$

$$\langle 3S | U_{OO} | 3S \rangle = -\frac{133}{16}\delta, \quad (\text{B8})$$

$$\langle 4S | U_{OO} | 4S \rangle = -\frac{27327}{1120}\delta, \quad (\text{B9})$$

for both the spin-singlet and -triplet states, and

$$\langle 1^{2S+1}S_S | U_{SS} | 1^{2S+1}S_S \rangle = \nu h_M^2 \delta, \quad (\text{B10})$$

$$\langle 2^{2S+1}S_S | U_{SS} | 2^{2S+1}S_S \rangle = \frac{5}{3} \nu h_M^2 \delta, \quad (\text{B11})$$

$$\langle 3^{2S+1}S_S | U_{SS} | 3^{2S+1}S_S \rangle = \frac{247}{120} \nu h_M^2 \delta, \quad (\text{B12})$$

$$\langle 4^{2S+1}S_S | U_{SS} | 4^{2S+1}S_S \rangle = \frac{83}{35} \nu h_M^2 \delta, \quad (\text{B13})$$

where

$$\delta = \frac{8\alpha_s K}{9\pi F(m_1 + m_2)}, \quad \xi = \frac{(M_0^{(0)})^2}{\Omega}, \quad (\text{B14})$$

$(M_0^{(0)})^2$ and Ω are defined by Eqs. (3.5a) and (3.5b), respectively, and ν is -3 (1) for $S=0$ ($S=1$).

For the pure orbitally excited states, the Coulomb-type, orbit-orbit-like, tensor, spin-orbit, and spin-spin potentials, U_C , U_{OO} , U_{SO} , U_T , and U_{SS} , contribute to their matrix elements. They are generally given by

$$\langle 1L | U_C | 1L \rangle = -\frac{3(L!)}{(2L+1)!!} \delta(\xi+L), \quad (\text{B15})$$

$$\langle 1L | U_{OO} | 1L \rangle = -\frac{3[(L+1)!]}{(2L+1)!!} \delta, \quad (\text{B16})$$

for both the spin-singlet and -triplet states,

$$\langle 1^3L_J | U_{SO} | 1^3L_J \rangle = \begin{cases} -\frac{3(L+1)^2[(L-1)!]}{(2L+1)!!} h_M \delta & \text{for } J=L-1, \\ -\frac{3(L+1)[(L-1)!]}{(2L+1)!!} h_M \delta & \text{for } J=L, \\ \frac{3(L+1)(L!)}{(2L+1)!!} h_M \delta & \text{for } J=L+1, \end{cases} \quad (\text{B17})$$

$$\langle 1^3L_J | U_T | 1^3L_J \rangle = \begin{cases} -\frac{(L+1)[(L-1)!]}{2(2L-1)[(2L+1)!!]} [3+L(L+3)] h_M^2 \delta & \text{for } J=L-1, \\ \frac{(L-1)!}{2[(2L+1)!!]} [3+L(L+3)] h_M^2 \delta & \text{for } J=L, \\ -\frac{L!}{2[(2L+3)!!]} [3+L(L+3)] h_M^2 \delta & \text{for } J=L+1, \end{cases} \quad (\text{B18})$$

$$\langle 1^{2S+1}L_{L+S} | U_{SS} | 1^{2S+1}L_{L+S} \rangle = -\frac{L(L!)}{2[(2L+1)!!]} \nu h_M^2 \delta, \quad (\text{B19})$$

and the matrix elements of the spin-orbit and tensor potentials for the spin-singlet states vanish.

For the radially excited states with nonzero orbital angular momentum, the Coulomb-type, orbit-orbit-like, spin-orbit, tensor, and spin-spin potentials, U_C , U_{OO} , U_{SO} , U_T , and U_{SS} , contribute to their matrix elements. They are given, for the several lower excited states, by

$$\langle 2P | U_C | 2P \rangle = -\frac{11}{10} \delta(\xi + 3), \quad (\text{B20})$$

$$\langle 2D | U_C | 2D \rangle = -\frac{19}{35} \delta(\xi + 4), \quad (\text{B21})$$

$$\langle 3P | U_C | 3P \rangle = -\frac{309}{280} \delta(\xi + 5), \quad (\text{B22})$$

$$\langle 2F | U_C | 2F \rangle = -\frac{29}{105} \delta(\xi + 5), \quad (\text{B23})$$

$$\langle 2P | U_{OO} | 2P \rangle = -\frac{22}{5} \delta, \quad (\text{B24})$$

$$\langle 2D | U_{OO} | 2D \rangle = -\frac{19}{7} \delta, \quad (\text{B25})$$

$$\langle 3P | U_{OO} | 3P \rangle = -\frac{927}{140} \delta, \quad (\text{B26})$$

$$\langle 2F | U_{OO} | 2F \rangle = -\frac{58}{35} \delta, \quad (\text{B27})$$

for both the spin-singlet and -triplet states,

$$\langle 2^3P_J | U_{SO} | 2^3P_J \rangle = \begin{cases} -\frac{28}{5} h_M \delta & \text{for } J=0, \\ -\frac{14}{5} h_M \delta & \text{for } J=1, \\ \frac{14}{5} h_M \delta & \text{for } J=2, \end{cases} \quad (\text{B28})$$

$$\langle 2^3D_J | U_{SO} | 2^3D_J \rangle = \begin{cases} -\frac{39}{14} h_M \delta & \text{for } J=1, \\ -\frac{13}{14} h_M \delta & \text{for } J=2, \\ \frac{13}{7} h_M \delta & \text{for } J=3, \end{cases} \quad (\text{B29})$$

$$\langle 3^3P_J | U_{SO} | 3^3P_J \rangle = \begin{cases} -\frac{471}{70} h_M \delta & \text{for } J=0, \\ -\frac{471}{140} h_M \delta & \text{for } J=1, \\ \frac{471}{140} h_M \delta & \text{for } J=2, \end{cases} \quad (\text{B30})$$

$$\langle 2^3F_J | U_{SO} | 2^3F_J \rangle = \begin{cases} -\frac{8}{5} h_M \delta & \text{for } J=2, \\ -\frac{2}{5} h_M \delta & \text{for } J=3, \\ \frac{6}{5} h_M \delta & \text{for } J=4, \end{cases} \quad (\text{B31})$$

$$\langle 2^3P_J | U_T | 2^3P_J \rangle = \begin{cases} -\frac{29}{10} h_M^2 \delta & \text{for } J=0, \\ \frac{29}{20} h_M^2 \delta & \text{for } J=1, \\ -\frac{29}{100} h_M^2 \delta & \text{for } J=2, \end{cases} \quad (\text{B32})$$

$$\langle 2^3D_J | U_T | 2^3D_J \rangle = \begin{cases} -\frac{47}{84} h_M^2 \delta & \text{for } J=1, \\ \frac{47}{84} h_M^2 \delta & \text{for } J=2, \\ -\frac{47}{294} h_M^2 \delta & \text{for } J=3, \end{cases} \quad (\text{B33})$$

$$\langle 3^3P_J | U_T | 3^3P_J \rangle = \begin{cases} -\frac{2831}{840} h_M^2 \delta & \text{for } J=0, \\ \frac{2831}{1680} h_M^2 \delta & \text{for } J=1, \\ -\frac{2831}{8400} h_M^2 \delta & \text{for } J=2, \end{cases} \quad (\text{B34})$$

$$\langle 2^3F_J | U_T | 2^3F_J \rangle = \begin{cases} -\frac{362}{1575} h_M^2 \delta & \text{for } J=2, \\ \frac{181}{630} h_M^2 \delta & \text{for } J=3, \\ -\frac{181}{1890} h_M^2 \delta & \text{for } J=4, \end{cases} \quad (\text{B35})$$

$$\langle 2^{2S+1}P_J | U_{SS} | 2^{2S+1}P_J \rangle = -\frac{1}{20} \nu h_M^2 \delta, \quad (\text{B36})$$

$$\langle 2^{2S+1}D_J | U_{SS} | 2^{2S+1}D_J \rangle = -\frac{2}{21} \nu h_M^2 \delta, \quad (\text{B37})$$

$$\langle 3^{2S+1}P_J | U_{SS} | 3^{2S+1}P_J \rangle = -\frac{1}{336} \nu h_M^2 \delta, \quad (\text{B38})$$

$$\langle 2^{2S+1}F_J | U_{SS} | 2^{2S+1}F_J \rangle = -\frac{11}{126} \nu h_M^2 \delta, \quad (\text{B39})$$

and the matrix elements of the spin-orbit and tensor potentials for the spin-singlet states vanish.

¹For recent reviews, see, for example, J. L. Rosner, in *Techniques and Concepts of High Energy Physics*, proceedings of the NATO Advanced Study Institute, St. Croix, 1980, edited by T. Ferbel (Plenum, New York, 1981); in *Experimental Meson Spectroscopy—1983*, proceedings of the Seventh International Conference, Brookhaven, edited by S. J. Lindenbaum (AIP Conf. Proc. No. 113) (AIP, New York, 1984); A. A. Bykov, I. M. Dremin, and A. V. Leonidov, *Usp. Fiz. Nauk* **143**, 3 (1984) [*Sov. Phys. Usp.* **27**, 321 (1984)].

²For recent reviews, see, for example, A. J. G. Hey and R. L. Kelly, *Phys. Rep.* **96**, 71 (1983); D. Gromes, in *The Quark Structure of Matter*, proceedings of the Yukon Advanced

Study Institute, Yukon, Canada, 1984, edited by N. Isgur, G. Karl, and P. J. O'Donnell (World Scientific, Singapore, 1985); B. Diekmann, Bonn University Report No. BONN-HE-84-29, 1984 (unpublished). For works on the light-quark meson spectrum, see A. De Rújula, H. Georgi, and S. L. Glashow, *Phys. Rev. D* **12**, 147 (1975); J. F. Gunion and R. S. Willey, *ibid.* **12**, 174 (1975); D. B. Lichtenberg and J. G. Wills, *Phys. Rev. Lett.* **35**, 1055 (1975); R. Barbieri *et al.*, *Nucl. Phys.* **B105**, 125 (1976); H. J. Schnitzer, *Phys. Rev. D* **18**, 3482 (1978); *Nucl. Phys.* **B207**, 131 (1982); *Phys. Lett.* **117B**, 96 (1982); **134B**, 253 (1984); **149B**, 408 (1984); B. R. Martin and L. J. Reinders, *Nucl. Phys.* **B143**, 309 (1978); R. H. Graham

- and P. J. O'Donnell, Phys. Rev. D **19**, 284 (1979); M. Frank and P. J. O'Donnell, Phys. Lett. **133B**, 253 (1983); Phys. Rev. D **29**, 921 (1984); L. J. Reinders, Z. Phys. C **4**, 95 (1980); J. Dias de Deus, A. B. Henriques, and J. M. R. Pulido, *ibid.* **7**, 157 (1981); T. Barnes, *ibid.* **11**, 135 (1981); R. K. Bhaduri, L. E. Cohler, and Y. Nogami, Nuovo Cimento **65A**, 376 (1981); F. Schöberl, Z. Phys. C **15**, 261 (1982); S. Ono and F. Schöberl, Phys. Lett. **118B**, 419 (1984); S. Ono, Acta Phys. Polon. **B75**, 201 (1984); A. B. Henriques, Z. Phys. C **18**, 213 (1983); J. B. Choi, Phys. Rev. D **31**, 201 (1985).
- ³D. P. Stanley and D. Robson, Phys. Rev. D **21**, 3180 (1980); J. Carlson, J. Kogut, and V. R. Pandharipande, *ibid.* **27**, 233 (1983); **28**, 2807 (1983); S. Godfrey and N. Isgur, *ibid.* **32**, 189 (1985); S. Godfrey, *ibid.* **31**, 2375 (1985).
- ⁴S. Ishida, Prog. Theor. Phys. **46**, 1570 (1971); **46**, 1905 (1971); I. Sogami, *ibid.* **41**, 1352 (1969); K. Fujimura, T. Kobayashi, and M. Namiki, *ibid.* **43**, 73 (1970); **44**, 193 (1970); R. P. Feynman, M. Kislinger, and F. Ravndal, Phys. Rev. D **3**, 2706 (1971); R. G. Lipes, *ibid.* **5**, 2849 (1972); Y. S. Kim and M. E. Noz, *ibid.* **8**, 3521 (1973).
- ⁵For a recent review, see S. Ishida, in *Hadron Spectroscopy—1985*, proceedings of the International Conference, University of Maryland, edited by S. Oneda (AIP Conf. Proc. No. 132) (AIP, New York, 1985).
- ⁶S. Ishida and T. Sonoda, Prog. Theor. Phys. **70**, 1323 (1983); T. Takabayasi, Prog. Theor. Phys. Suppl. **67**, 1 (1979).
- ⁷S. Ishida *et al.*, Prog. Theor. Phys. **71**, 806 (1984).
- ⁸K. Yamada and S. Ishida, in *Hadron Spectroscopy—1985* (Ref. 5); K. Yamada, Doctoral thesis, Nihon University, 1984. This conference report contains errors in treating the spin-orbit interaction and the retardation effect, and they are corrected in this paper.
- ⁹S. Ishida, K. Yamada, and M. Oda, Phys. Rev. D **28**, 2918 (1983).
- ¹⁰A. Salam, R. Delbourgo, and J. Strathdee, Proc. R. Soc. London **A284**, 146 (1965); B. Sakita and K. C. Wali, Phys. Rev. **139**, B1355 (1965).
- ¹¹S. Ishida, A. Matsuda, and M. Namiki, Prog. Theor. Phys. **57**, 210 (1977).
- ¹²T. Takabayasi, Nuovo Cimento **33**, 668 (1964).
- ¹³Fujimura, Kobayashi, and Namiki (Ref. 4); S. Ishida *et al.*, Phys. Rev. D **20**, 2906 (1979).
- ¹⁴A. Duncan, Phys. Rev. D **13**, 2866 (1976); H. J. Schnitzer, Phys. Lett. **65B**, 239 (1976); Lai-Him Chan, *ibid.* **71B**, 422 (1977).
- ¹⁵H. J. Schnitzer, Phys. Lett. **69B**, 477 (1977); Phys. Rev. D **18**, 3482 (1978); **19**, 1566 (1979).
- ¹⁶For similar attempts, see S. Blaha, Phys. Rev. D **10**, 4268 (1974); Phys. Lett. **56B**, 373 (1975); Y. S. Kim, Phys. Rev. D **14**, 273 (1976); M. J. Ruiz, *ibid.* **30**, 683 (1984); A. O. Barut and S. Komy, Fortschr. Phys. **33**, 309 (1985).
- ¹⁷Particle Data Group, Rev. Mod. Phys. **56**, S1 (1984).
- ¹⁸H. Aihara *et al.*, Phys. Rev. Lett. **53**, 2465 (1984). See also H. Albrecht *et al.*, Phys. Lett. **146B**, 111 (1984); A. E. Asratyan *et al.*, *ibid.* **156B**, 441 (1985).
- ¹⁹K. Han *et al.*, Phys. Rev. Lett. **55**, 36 (1985).
- ²⁰If the oscillator constant K is taken to be flavor independent as in the standard potential models motivated by QCD, this regularity is obtained by simply assuming the constant F to be also flavor independent. Recently the possibility of deriving this regularity in the potential models motivated by QCD was discussed: K. Igi and S. Ono, Phys. Rev. D **32**, 232 (1985); M. Frank and P. J. O'Donnell, Phys. Lett. **159B**, 174 (1985).
- ²¹B. Alper *et al.*, Phys. Lett. **94B**, 422 (1980).
- ²²D. L. Denney *et al.*, Phys. Rev. D **28**, 2726 (1983).
- ²³D. Aston *et al.*, Phys. Lett. **149B**, 258 (1984); Nucl. Phys. **B247**, 261 (1984).
- ²⁴C. Daum *et al.*, Nucl. Phys. **B187**, 1 (1981).
- ²⁵A possibility is pointed out that two unestablished resonances $\rho(1250)$ and $K^*(1410)$ may be assigned, respectively, to the first radial excited states of $\rho(770)$ and $K^*(892)$ (see Ref. 23). However, these assignments seem unnatural from a standard quark potential model, considering that the masses of these mesons are in the same range as those of the $1P$ multiplets. We feel that these mesons might be interpreted as four-quark or hybrid states.
- ²⁶As for attempts to overcome this difficulty, see, for example, H. Leutwyler and J. Stern, Phys. Lett. **73B**, 75 (1978); Nucl. Phys. **B157**, 327 (1979); J. Jersák, H. Leutwyler, and J. Stern, Phys. Lett. **77B**, 399 (1978); J. Jersák and D. Rein, Z. Phys. C **3**, 339 (1980); T. Takabayasi, Prog. Theor. Phys. **61**, 1235 (1979); I. Sogami and H. Yabuki, Phys. Lett. **94B**, 157 (1980); see also Ref. 28.
- ²⁷L. P. Horwitz and F. Rohrlich, Phys. Rev. D **31**, 932 (1985); H. Sazdjian, Phys. Lett. **156B**, 381 (1985).
- ²⁸H. W. Crater and P. Van Alstine, Ann. Phys. (N.Y.) **148**, 57 (1983); Phys. Rev. Lett. **53**, 1527 (1984).